USE OF MATRICES FOR THE ADAPTATION OF VIDEO-BASED PHOTOGONIOMETRIC MEASUREMENTS TO A VARIABLE REFERENTIAL

M. Andersen

Solar Energy and Building Physics Laboratory LESO-PB, Swiss Federal Institute of Technology EPFL, CH – 1015 Lausanne, Switzerland

ABSTRACT

Digital video based luminance mapping systems require the establishment of a precise relation between the considered spatial referential and the associated pixel coordinates on the image, that may vary with the measurement conditions. In this paper, an adaptation of the image calibration according to the referential variations is proposed, based on the use of a set of matrices individually associated to each spatial coordinate. This approach is given through an application example on a recent digital imaging-based bi-directional photogoniometric device.

RESUME

Les systèmes de mesure de luminance basées sur l'imagerie numérique nécessitent une relation précise entre le référentiel considéré et les coordonnées des pixels associés sur l'image, qui peut varier avec les conditions de mesure. Ce papier propose une adaptation du calibrage de l'image en fonction des variations de référentiel, à l'aide d'un ensemble de matrices individuellement associées à chaque coordonnée spatiale. Cette approche est illustrée par une application sur un photogoniomètre bidirectionnel, basé sur l'imagerie numérique.

INTRODUCTION

A way to solve the problem of geometric calibration for a digital imaging based luminance-meter with variable referential appears when the latter undergoes geometric transformations that are analytically characterisable, even with non linear consequences on the image, provided that the relative positions of the camera and the filmed objects remain unchanged. The recognition and geometrical characterisation of objects on images aiming to deduce spatial parameters [1] is indeed not the subject treated here; this paper proposes a method to analyse images of a known geometric situation, whose investigation provides the expected information about a particular feature, bi-directional light transmission in our case, other photometric [2] or extended applications, and it is the observed feature that may be related to a well-known but variable referential.

The exposed method consists of using a set of matrices, whose dimensions are equal to the pixel resolution of the digital images, and which are composed of spatial coordinates describing the system, each coordinate being associated to a different matrix. The referential transformations can thus be applied by calculating the associated modifications on the matrices, which are then taken as a basis to adapt the image geometric calibration.

In order to extensively illustrate this approach, we will use a concrete case of using digital imaging for photometric measurements, where referential variations are present: the bi-directional photogoniometer developed at the Solar Energy and Building Physics Laboratory (LESO-PB, EPFL) for light transmission measurements. Details on its calibration procedures, image and data processing and results can be found in [3].

GENERAL PROBLEM STATEMENT

The functioning principle of the bi-directional photogoniometer developed at the LESO-PB, EPFL and based on digital imaging techniques is the following: the light source being fixed, an inclination of the photogoniometer combined to a rotation of the sample holder determines the incident direction (θ_1, ϕ_1), θ for altitude and ϕ for azimuth (see Fig. 1B); a rotating ring moving underneath the main platform and on which the CCD camera and a projection screen are fixed allows a complete visualisation of the transmitted light within six 60° rotations.

As illustrated on Figure 1A, the intuitive approach consisting of an observation of the transmitted light on a hemispherical surface with a mobile sensor is replaced by a projection of the transmitted light on a diffusing triangular panel. The latter reflects the light towards the CCD camera, which provides a picture of the whole screen. After six rotations of this system, with image capture and calibration at each position, the transmitted light distribution is fully known.

The spatial referential is given in spherical coordinates, which is the most intuitive representation of light transmission behaviour. As illustrated on Fig. 1B, the base plane for incidence ($\theta_1 = 90°$, $\phi_1 \in [0°;360°[$) is given by the external sample interface, which is fixed; the base plane for transmission ($\theta_2 = 90°$, $\phi_2 \in [0°;360°[$) is given by the internal sample interface, whose geometrical properties thus vary with the sample thickness, as detailed in next §. The azimuth origin axes $\phi_1 = 0°$ and $\phi_2 = 0°$ are bound to the sample itself; therefore, a rotation of the latter will induce a referential variation; this effect will be discussed below.

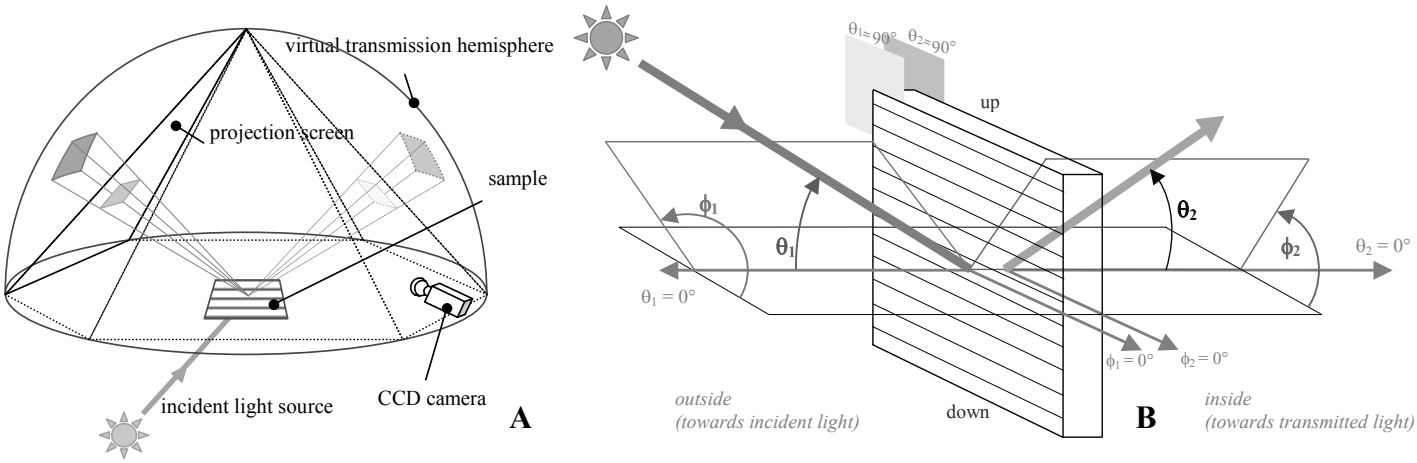

Figure 1: Bi-directional photogoniometer based on digital imagery. (A) Functioning principle. (B) Spatial referential for input (index 1) and output (index 2) coordinates.

The data provided by a bi-directional photogoniometer are bi-directional transmission distribution functions (BTDFs); as the measured quantities are screen luminances L_{screen} (θ_1, ϕ_1, θ_2, ϕ_2), BTDF values must be expressed according to it, and taking correction factors into account: distance d between sample and screen along direction (θ_2, ϕ_2), ray inclination α (angle between direction (θ_2, ϕ_2) and normal to screen), screen reflection coefficient ρ, incident illuminance $E_1(\theta_1)$, illuminated area A. This leads to equation (1) [3]:

$$BTDF\ (\theta_1,\phi_1,\theta_2,\phi_2)\left[\frac{cd}{m^2 \cdot lx}\right] = \frac{\pi}{\rho} \cdot \frac{d^2\,(\theta_2,\psi_2)}{A \cdot \cos\theta_2 \cdot \cos\alpha} \cdot \frac{L_{screen}\,(\theta_1,\phi_1,\theta_2,\phi_2)}{E_1\,(\theta_1)} \qquad (1)$$

In order to determine BTDF values according to a regular output resolution ($\Delta\theta_2$, $\Delta\phi_2$), outgoing zones have to be defined around the considered directions (θ_2, ϕ_2). The transmitted luminances being here measured on a projection screen, the latter must be divided into a certain grid of discretisation zones that depends on the output resolution desired (an example is shown on Fig. 4A for an output resolution ($\Delta\theta_2$, $\Delta\phi_2$) of (5°, 5°)).

REFERENTIAL VARIATIONS

Before considering the spatial variations, a reference case is chosen, in order to establish the possible modifications in comparison to it. This reference situation corresponds to a sample thickness e = 7.5cm, which leads to an internal sample interface (i.e. plane ($\theta_2 = 90°$, $\phi_1 \in [0°;360°[$)) including the projection triangle base (cf. Fig. 2).

Let us consider the geometric calibration in three phases: first an analysis of an arbitrary screen position in order to associate pixel coordinates (X, Y) on the image to angular quantities (θ_{2Ref}, ψ_2) based on the reference situation (index "Ref"); then their correspondence to real screen angles (θ_2, ψ_2), taking the sample thickness into account (see next §); finally, their conversion into spherical coordinates (θ_2, ϕ_2) defined for the whole hemisphere, detailed below, which depends on the screen position concerned and on the incident azimuth angle ϕ_1.

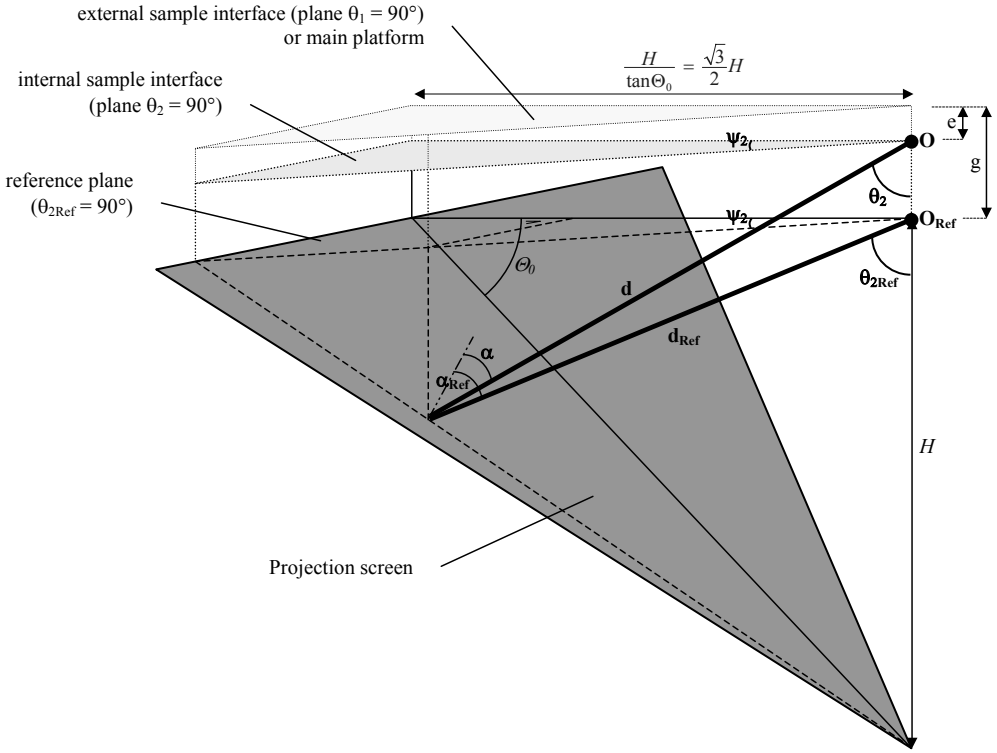

Figure 2: Relation between polar co-ordinates (θ_2, ψ_2) and reference coordinates (θ_{2Ref}, ψ_2). g = 7.5cm represents the distance between the external sample interface and the triangle base plane. The reference situation corresponds to a sample thickness e equal to g.

Translation with sample thickness

The correspondence between (θ_{2Ref}, ψ_2) and (θ_2, ψ_2) depends on the sample thickness e, and on other quantities that are fixed: gap g between external sample interface and triangle base plane, distance H, angle Θ_0. As far as the image is concerned, the screen will certainly keep its shape and position on the picture whatever sample thickness is taken, but the same pixel may represent different altitude angles θ_2. Fig. 4B shows the superposition of a discretisation grid corresponding to e = 7.5cm (reference situation) over the pattern of zones associated to e = 0: it

can be observed that the influence of sample thickness can be considerable on geometric calibration, especially for growing values of θ_2. In order to adapt the geometric calibration through matrix calculations, as explained further, θ_2 and d must be known as functions of (q_{2Ref}, ψ_2, and d_{Ref}), leading to equation (2):

$$\theta_2 = \arcsin\frac{d_{Ref}\cdot\sin\theta_{2Ref}}{d} = \arcsin\frac{d_{Ref}\cdot\sin\theta_{2Ref}}{\sqrt{\left(d_{Ref}\cdot\cos\theta_{2Ref}+(g-e)\right)^2+\left(d_{Ref}\cdot\sin\theta_{2Ref}\right)^2}} \qquad (2)$$

Rotation with azimuth angle of incident beam

Each screen image has to be considered as being part of a global combination that recreates the transmission hemisphere according to six complementary planar projections (cf. Fig. 1A). The grid of outgoing zones has thus to be understood as a discretisation of the whole transmission hemisphere. The meshes dimensions are proportional to the chosen output steps $\Delta\theta_2$ and $\Delta\phi_2$; their spatial disposition depends on the incident azimuth ϕ_1. Indeed, a changing in incidence azimuth is concretised by a rotation of the sample itself, to which the output referential is linked (cf. Fig. 1B); the six screen positions remaining fixed, such a rotation imposes a simultaneous turning around of the applied discretisation grid. This implies that the origin axis for ϕ_2 - and the screen position number n_{e0} on which it is projected - are directly associated to the ϕ_1 value (see Fig. 3). Two types of situations need to be solved: either ϕ_1 is a multiple of $\Delta\phi_2$, or not. Let us note that $\Delta\phi_2$ is required to be a divisor of 60°.

As observed on Fig. 4B, if the sample's rotation angle ϕ_1 is a multiple of the azimuth angle step $\Delta\phi_2$, the spatial distribution of the different discretisation zones will remain unchanged, whereas the azimuth angles ϕ_2 which they each correspond to will depend on the exact value of ϕ_1. n_{e0} is a critical parameter for the outgoing azimuth angles: it comprises the "starting line" for ϕ_2. On the example illustrated by Fig. 4B, with ϕ_1 = 75°, the zones where ϕ_2 = 0° correspond to the zones ψ_2 = -15° of screen position n_{e0} = 1; this particular value of ψ_2 is named $\psi_{2:\phi0°}$. The relation between ϕ_2 and ψ_2 is given by equation (3):

$$\phi_2 = (\Delta n_{e0}\cdot 60° + \psi_2 - \psi_{2:\phi0°} + 360°) \text{ modulo } 360° \qquad (3)$$

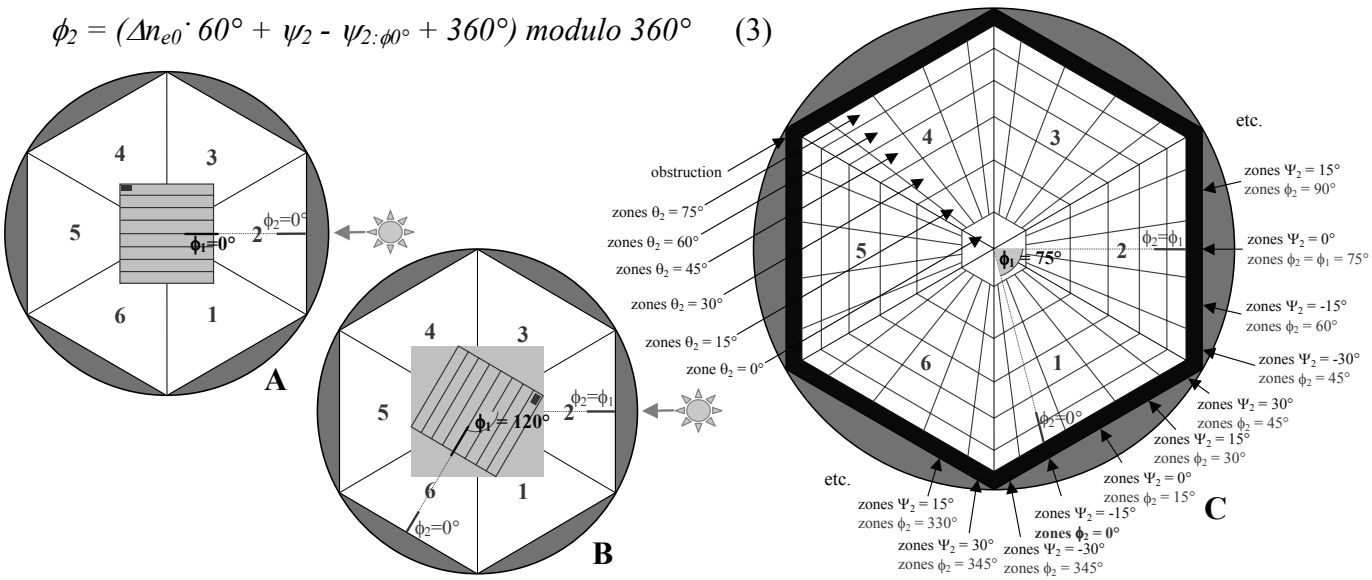

Figure 3: (A) and (B) Orthogonal projection view of the sample orientation superimposed to the six screen positions. (A) ϕ_1 = 0° i.e. default sample orientation; (B) ϕ_1 = 120°. (C) Schematised global discretisation grid ($\Delta\theta_2$, $\Delta\phi_2$) = (15°, 15°) for ϕ_1 = 75°.

In the case ϕ_1 is not a multiple of $\Delta\phi_2$, the shift in azimuth does not correspond to entire grid steps; analytical conversions from screen to global coordinates based on the default discretisation grid are therefore not anymore adapted to investigate such incidence situations. At the level of the screen itself, a new individual grid has to be built, as can be observed on Fig. 4C. It can be noted that the effective shift $S\phi_1$ between any discretisation grid and the corresponding default one is equal to ϕ_1 modulo $\Delta\phi_2$, and the creation of a wholly new grid is only necessary if the latter is of non-zero value, analytical conversions being from then insufficient to adapt the discretisation.

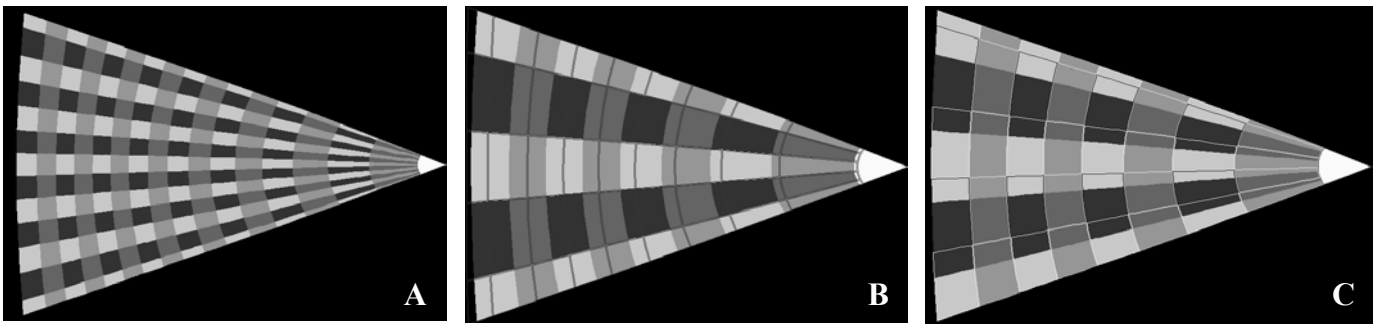

Figure 4: (A) Discretisation zones for ($\Delta\theta_2$, $\Delta\phi_2$) = (5°, 5°). (B) and (C): Superposition of grids for ($\Delta\theta_2$, $\Delta\phi_2$) = (10°, 15°). (B) e = 7.5cm (borders) over e = 0 (pattern); (C) ϕ_1 = 50° (borders) over ϕ_1 = 0° (default pattern), displaying a 5° shift (=ϕ_1 modulo $\Delta\phi_2$) in azimuth.

METHODOLOGY AND SOFTWARE IMPLEMENTATION

The problem statement being established, a particular image processing is developed in order to adequately integrate the exposed referential variations for the BTDF assessment. As explained above, the general methodology consists of considering the digital image as a rectangular (n x m) array of data, and expressing the spatial coordinates as (n x m) matrices, each one being composed of angular or distance coefficients individually associated to the corresponding pixels on the image. The matrix coefficients must then be gathered into discretisation zones, according to their respective values and to the referential conditions; the different processing phases, necessary to achieve an appropriate extraction of BTDF data and executed by MATLAB® (v. 5.3, The MathWorks, Inc.) are given below.

From a set of known marks, drawn on the projection screen and manually located on its image in order to be associated to their pixel coordinates (X, Y), a pair of complete matrices of angular values θ_{2Ref} and ψ_2 are created, called $M\theta_{2Ref}$ and $M\psi_2$, providing these coordinates for every pixel of the screen image after interpolation. The obtained matrices are used as a calculation basis for referential variations, which allows a reliable integration of image distortions even for variable situations. Indeed, the aberrations are taken into account at the very first step of processing, and are then transmitted without any alteration when the geometric parameters, exclusively presenting wholly analytical variations, are modified.

The real altitude angle distribution $M\theta_2$ for a given sample thickness e is calculated through equation (2); its elements are gathered through the creation of a new set of binary matrices named "GroupTheta(θ_2)", where θ_2 increases from 0° with $\Delta\theta_2$ steps from one matrix to another, each one being composed of ones where the corresponding $M\theta_2$ coefficients are comprised between ($\theta_2 - \frac{1}{2}\Delta\theta_2$) and ($\theta_2 + \frac{1}{2}\Delta\theta_2$), and of zeros elsewhere. As far as the azimuth variation is concerned, once the set of new discretisation grids is defined, each one being associated to a different effective shift situation $S\phi_1$, the corresponding azimuth matrices can be built. The new azimuth values have first to be determined for each pixel, as the applied $S\phi_1$ shift will alter the gathering into zones. Matrix $M\psi_2$ is therefore converted into a "shifted"

matrix $M\psi'_2\_(S\phi_1)$ whose coefficients are defined by $\psi'_2 = \psi_2 + S\phi_1$ for each shift situation, the addition being chosen in order to adapt the values according to the clockwise increase of ϕ_1 over the screen positions (cf. Fig. 3). The coefficients of $M\psi'_2\_(S\phi_1)$ are thus connected to a kind of hybrid situation taking the effective shift into account while still defined for an arbitrary screen position. Based on arrays $M\psi'_2\_(S\phi_1)$, a set of binary matrices named "GroupPsi(ψ'_2)_($S\phi_1$)" can be created, each one being composed of 1 where the corresponding pixels are associated to discretisation zones ψ'_2 and shift situation $S\phi_1$.

Once all the matrices GroupTheta(θ_2) and GroupPsi(ψ'_2)_($S\phi_1$) are created, their element-per-element multiplication according to pairs of values θ_2, ψ'_2 will determine the different discretisation zones (θ_2, ψ'_2), for each shift situation $S\phi_1$ and an arbitrary screen position. During a sample characterisation, at each screen position and after image acquisition, grey level to luminance calibration, division by illuminance, and combination into a final, fully calibrated 32 bits image [3], a matrix "MLscreenE" is created, corresponding to the array of screen luminance values per lux given by the actual final image pixels. After correcting these $L_{screen} / E_1(\theta_1)$ values into BTDF data through equation (1), leading to a matrix "MBTDF", the discretisation into outgoing zones is performed according to a loop sequence, where matrix MBTDF is in turn multiplied by the different zone matrices resulting from GroupTheta(θ_2) .˙ GroupPsi(Existψ'_2(ψ'_2))_($S\phi_1$), for each (θ_2, ψ'_2) zone couple and for the actual shift situation ($S\phi_1$) and where the average BTDF value of the concerned zone is calculated at each run.

Once all the BTDF values have been extracted, they must be associated to their respective couple (θ_2, ϕ_2). As θ_2 is directly given by matrix $M\theta_2$, this amounts to find ϕ_2 by solving equation (3), and therefore to estimate variables $\psi_{2:\phi 0°}$ and Δn_{e0}.

CONCLUSION

A new method for adapting geometric calibration for digital image-based photogoniometric measurements with variable referential has been exposed. Such a procedure aims to adjust the analysis of a particular feature in a known geometric situation, the observed feature being related to a spatial referential that might change. This method lies on the use of matrix calculations, in order to provide flexibility in output resolution, and a precise rectification of the coordinate system according to the referential parameters. Reciprocal transformations from images, considered as a (n x m) arrays of data, to matrices allow accurate geometric adaptations and an appropriate and flexible gathering into discretisation zones, required for a BTDF assessment relative to a particular output resolution.

The procedure, developed within the framework of BTDF measurements achieved by a digital imaging based transmission photogoniometer, has been revealed performing and efficient, providing reliable BTDF results within only 2 to 4 minutes per incident direction. It has moreover proven to be very stable even for extreme resolutions or hard referential variations.

REFERENCES

1. Tao, C.V.: Semi-automated object measurement using multiple-image matching from mobile mapping image sequences. Photogr. Eng. and Remote Sens., vol 66 (12), pp. 1477-1485, 2000.
2. Song, K.D. et al.: Determining Daylighting Parameters by a Luminance Mapping System and Scale Models. IESNA, vol. 23 (1), pp. 65-75, 1994.
3. Andersen, M. et al.: Experimental assessment of bi-directional transmission distribution functions using digital imaging techniques. Energy & Buildings, vol 33 (5), pp. 417-431, 2001.